J Infrared Milli Terahz Waves (2011) 32:691–698
DOI 10.1007/s10762-010-9645-9

Terahertz Spectroscopy of Histidine Enantiomers and Polymorphs

Alan B. True · Konstanze Schroeck · Timothy A. French · Charles A. Schmuttenmaer

Received: 25 January 2010 / Accepted: 20 April 2010 /
Published online: 22 May 2010

Abstract We have measured terahertz and powder x-ray diffraction spectra of D-histidine, L-histidine, and DL-histidine. The as-received D and L material exists in two different polymorphs: D-histidine is in the metastable monoclinic form, while L-histidine is in the stable orthorhombic form. For both the L and D enantiomers, recrystallization of the as-received material results in a mixture of the monoclinic and orthorhombic forms.

Keywords Histidine · Polymorphism · THz

1 Introduction

Polymorphism has long been an important issue in solid state chemistry and the pharmaceutical industry. Polymorphs are different crystal structures of the same molecular material. Within the pharmaceutical industry, important physical properties such as solubility and bioavailability are dependent on the product's morphology [1–6]. In turn, the manufacturing process is governed by the physical properties of the product's morphology in terms of its solubility, melting point and reactivity.

Terahertz time-domain spectroscopy (THz-TDS) has become a useful tool for morphology determination. Although other techniques exist, including x-ray crystallography and Raman spectroscopy, THz spectroscopy is a simple and effective method that probes the spectral region of 0.1–3 THz where the crystal librations arising from the lattice structure are found [7, 8]. These are in addition to modes that are of mixed *inter*molecular

A. B. True · K. Schroeck · T. A. French · C. A. Schmuttenmaer (✉)
Department of Chemistry, Yale University, P.O. Box 208107, 225 Prospect St., New Haven, CT 06520-8107, USA
e-mail: charles.schmuttenmaer@yale.edu

Present Address:
T. A. French
Department of Chemistry and Chemical Biology, Harvard University, 1 Oxford Street, Cambridge, MA 02138, USA

and *intra*molecular character, particularly at in the higher frequency range. Despite the fact that the THz spectrum is a direct description of the phonon modes of a crystalline state, only limited work has been done with THz spectroscopy to explore polymorphism [9–12]. Applying THz spectroscopy to some important and well studied polymorphs demonstrates the technique's ability to quickly and clearly differentiate between them.

The general conclusions of previous work with amino acids are that crystals of D and L enantiomers of a particular molecule have identical spectra while the racemate has a unique spectrum [13]. This is because the optical isomers can crystallize in the same configuration (with opposite handedness) and the DL racemate necessarily has a different lattice structure. This also demonstrates conclusively that the modes found in these spectra are significantly intermolecular in nature as any intramolecular modes would be necessarily common to both spectra.

Polymorphs of some amino acids such as L-serine, L-cysteine and L-histidine are known to exist under ambient temperature/pressure conditions [14], and polymorphism is a common issue for organic solids, and thus the utility of THz spectroscopy is clearly not limited to amino-acids or biomolecules.

In their crystallization and polymorphism study, Roeland *et al.* report only two crystalline forms of L-histidine, a stable orthorhombic form and a metastable monoclinic form [15]. Additionally, only the monoclinic [16] and orthorhombic [17] morphologies of L-histidine are listed on the Cambridge Structural Database (CCD) [18]. From this information, and the lack of any other reported morphology, it is presumed that only these two polymorphs of L or D-histidine are involved in our study.

Polycrystalline samples of D, DL, and two morphologies of L-histidine are characterized and investigated by THz spectroscopy. The atomic coordinates of the DL-histidine structure and both of the morphologies of L and D-histidine are cataloged in the CCD. These coordinates are used to calculate their theoretical powder patterns with Mercury 1.4.1 software [19]. Experimental powder diffraction patterns of the two L-histidine polymorphs are compared to the calculated patterns of the two known morphologies, allowing us to determine that the L sample is in the stable orthorhombic form, while the D sample is in the metastable monoclinic form. We also find that the recrystallized L and D samples are an approximate 50%-50% mixture of the orthorhombic and monoclinic forms.

2 Experimental

The THz beam is produced by a regeneratively amplified Ti:Sapphire laser with a repetition rate of 1 kHz, center frequency of 790 nm, pulse duration of 100 fs, and pulse energy of 600 μJ. The beam is split with the majority of the power impinging on a ZnTe(110) crystal to generate THz radiation by optical rectification [20, 21]. The remainder of the beam is delayed using a motorized translation table and is used as a detection gate by means of free space electro-optic sampling [22]. The THz region of the spectrometer is purged with nitrogen to reduce ambient water vapor absorption. The time-domain of the THz electric field is collected; the Fourier transform gives the spectral absorption and the index of refraction. A complete description has been published previously [23].

The histidine samples were purchased from Sigma-Aldrich and crushed with a mortar and pestle to obtain uniformity of about 5 to 15 μm grain size. The sample powder was then pressed into a 13 mm diameter pellet at a pressure of 680 atm. Sample thicknesses were on the order of 0.2–0.5 mm. Low temperature measurements are carried out with a Janis optical cryostat using Mylar windows to minimize distortion of the THz pulse.

A simple solvent evaporation is used for the recrystallization of histidine samples. Samples are dissolved in a sufficient amount of water; occasionally the solution is modestly heated until the samples are completely dissolved. The solutions are allowed to evaporate at room temperature until dry. The resultant precipitate is prepared in the same fashion as the as-received Sigma-Aldrich samples.

The powder diffraction patterns were performed on a Brucker-AXS D8 Focus. The diffractometer uses a copper source to generate 1.54 Å radiation. Samples are scanned with a step size of 0.020°, a step time of 2 seconds, a divergence of 0.6 mm, anti-scatter of 0.6 mm, and a detector slit width of 0.1 mm.

3 Results and discussion

3.1 Enantiomeric histidine THz spectra

Figure 1 displays the zwitterionic form of L and D-histidine. The zwitterionic form is chosen because that is the form found in the crystals. Each of the three solids (as received from Sigma-Aldrich) results in a unique THz spectrum (Fig. 2a). Upon recrystallization of all three solids, the spectra of D and L-histidine are different from the as-received material, but now they each have the same spectrum as each other (Fig. 2b). The DL-histidine spectrum remains unchanged. The fact that the D and L spectra are different from each other has not been reported previous work with amino acids. The recrystallized sample spectra in Fig. 2b are more consistent with previous work, in that the D and L enantiomers have similar spectra while the DL racemate is different.

Figure 2c compares the recrystallized D and L spectra from Fig. 2b with a spectrum generated by taking a 50%-50% linear combination of the as-received spectra. This indicates that the two as-received samples are each a single polymorph, while the recrystallized sample is a mixture. If one of the as-received samples were a mixture of polymorphs and the recrystallized sample were pure, then the pure as-received spectrum would have to be subtracted from the mixture spectrum to obtain the recrystallized spectrum, which is clearly not the case.

Not only did Roeland's crystallization and polymorphism study report two crystalline forms, they also found that the ratio of polymorphs could be varied by varying crystallization conditions [15]. Therefore, it is seen that Sigma-Aldrich uses different crystallization conditions for their L and D material, which are both different than the recrystallization conditions that we employed.

3.2 X-ray powder diffraction data

While the THz spectra unambiguously capture the fact that the different samples have different polymorphs, x-ray diffraction powder patterns are needed to assign the polymorph to each spectrum.

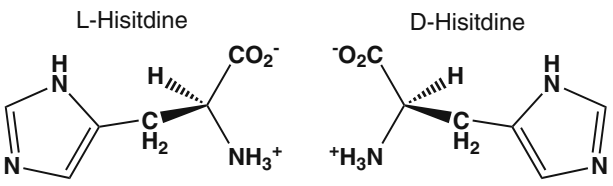

Fig. 1 Zwitterionic form of Histidine enantiomers.

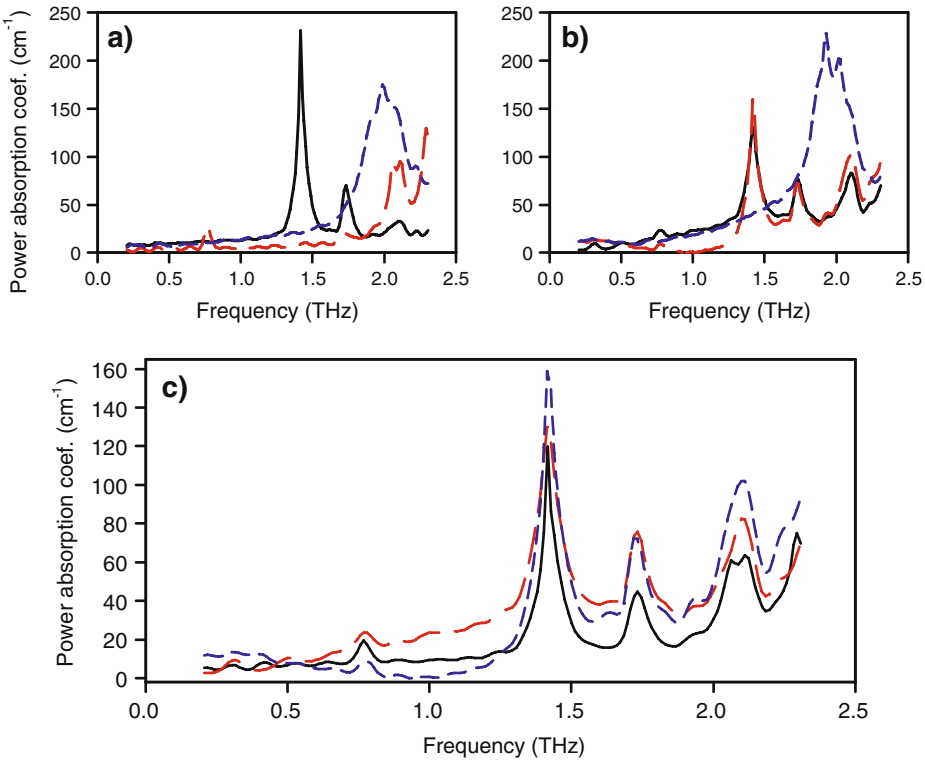

Fig. 2 THz spectra of enantiomers and polymorphs of histidine. Data from the Sigma-Aldrich samples shows three unique morphologies (part a). The black solid line is D-histidine, the red long-dashed line is L-histidine, and the blue short-dashed line is DL-histidine. Part b) Upon recrystallization, the D and L sample have identical spectra, while DL has not changed (colors and line styles are the same as in part a). Part c) compares a spectrum comprised of a 50%-50% linear combination of the D and L-histidine spectra in part a), shown with the black solid line, with the spectra of recrystallized D and L-histidine (red long-dashed and blue short-dashed lines, respectively).

It is known from the literature, that L-histidine exists either in the orthorhombic crystal system (space group $P2_12_12_1$) or in the monoclinic crystal system (space group $P2_1$) [15, 24, 25]. The conformations in both forms are stabilized via an intramolecular hydrogen bond between a hydrogen atom in the amino group and a nitrogen atom in the imidazole ring. DL-histidine crystallizes in the monoclinic crystal system, but in the centrosymmetric space group $P2_1/c$ [26].

Figure 3 displays the XRD powder diffraction data for as-received L-histidine and D-histidine, as well as that for recrystallized L-histidine. In addition, calculated powder patterns for the orthorhombic and monoclinic polymorphs are shown. The unit cell parameters are given in Table 1. The stable orthorhombic form is LHISTD13, and the metastable monoclinic form is LHISTD04.

A difficulty with powder XRD spectra is that the intensities depend strongly on sample preparation and are not quantitative. This is seen most strikingly in the right panel of Fig. 3 where a linear scale is used for the intensity. However, when plotted using a logarithmic intensity scale (left side of Fig. 3), it becomes possible to assign the measured spectra to the calculated ones, keeping in mind that peak positions are more important than peak intensities.

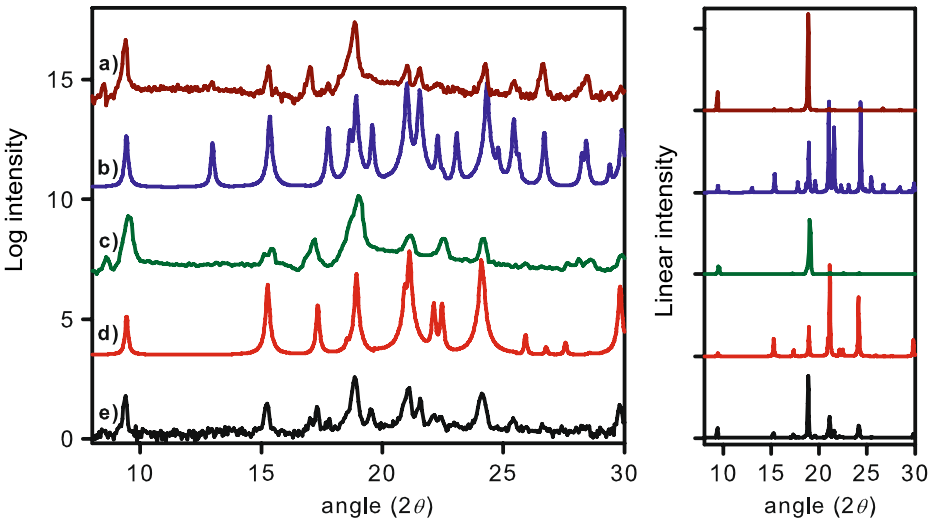

Fig. 3 Left side shows XRD powder patterns of a) L-histidine, b) the calculated spectrum of the orthorhombic form of L-histidine (LHISTD13), c) D-histidine, d) the calculated spectrum of the monoclinic form of L-histidine (LHISTD04), and e) recrystallized L-histidine. They are plotted on logarithmic scale. Spectra have been offset in increments of 3.5 for clarity. Right side shows the same spectra plotted on a linear scale.

Parts a) and c) of Fig. 3 are the spectra of the as-received L and D-histidine, respectively. Parts b) and d) are the calculated powder patterns for the stable orthorhombic and metastable monoclinic polymorphs, respectively. Clearly, the as-received L-histidine is the orthorhombic polymorph and the as-received D-histidine is the monoclinic polymorph. Part e) is the powder XRD spectrum of recrystallized L-histidine. It is known from the THz work that it is a 50%-50% mixture of the two polymorphs, but that is not readily apparent in part e) of Fig. 3. However, Fig. 4 presents the experimentally measured spectrum from Fig. 3, along with a 50%-50% linear combination of the as-received spectra (parts a) and c) in Fig. 3). Within the limits of powder XRD data quality, there is a very good match which further supports the conclusions from the THz work.

3.3 Low temperature THz spectra

The THz spectrum of L-histidine is reported by Rungsawang *et al*. and is identified as the orthorhombic polymorph [27]. This agrees with our assignment of the morphology.

Table 1 Unit cell parameters for DL-histidine and two L-histidine polymorphs.

Cambridge Database Identifier	Temp.	Space Group	Cell Lengths (Å)			Cell Angles		
			a	b	c	α	β	γ
LHISTD04	295	$P2_1$	5.166	7.385	9.465	90	98.16	90
LHISTD13	295	$P2_12_12_1$	5.175	7.315	18.750	90	90	90
DLHIST	295	$P2_1/c$	8.983	8.087	9.415	90	97.65	90

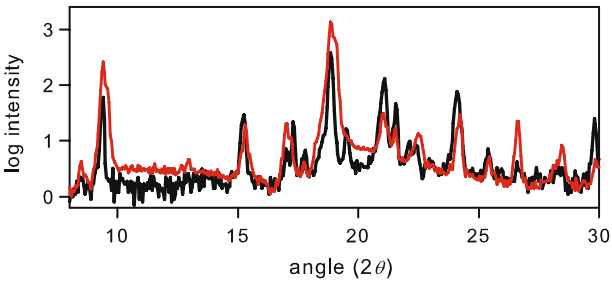

Fig. 4 XRD powder patters for recrystallized L-histidine (thick black line) and 50%-50% linear combination of L-histidine and D-histidine (thin red line).

Low temperature data were collected to investigate the peak positions and shapes (Fig. 5). Most spectra have the same general behavior at low temperature; the peaks tend to blue-shift relative to room temperature. D-histidine demonstrates this trend well at low temperature, all peaks shift about 0.04 THz to higher frequency (Fig. 5b). L-histidine does not have such a pronounced shift at low temperature (Fig. 5a) but DL-histidine shows a moderate shift of all three peaks in its spectrum (Fig. 5c). These shifts may be a result of an anharmonicity in the potential energy surface, but are most likely dominated by changes in the potential energy surface due to thermal contraction or expansion. As in a harmonic oscillator, a more highly curved potential surface results in a higher transition frequency.

4 Conclusions

The THz spectra of polycrystalline L and D-histidine enantiomers and the DL-histidine racemate are reported. The fact that each sample has a unique spectrum (prior to recrystallization) demonstrates the strength of THz spectroscopy in the area of polymorphism. Samples of the polymorphs are recrystallized using simple solvent evaporation to convert the stable orthorhombic form of L-histidine into an approximate

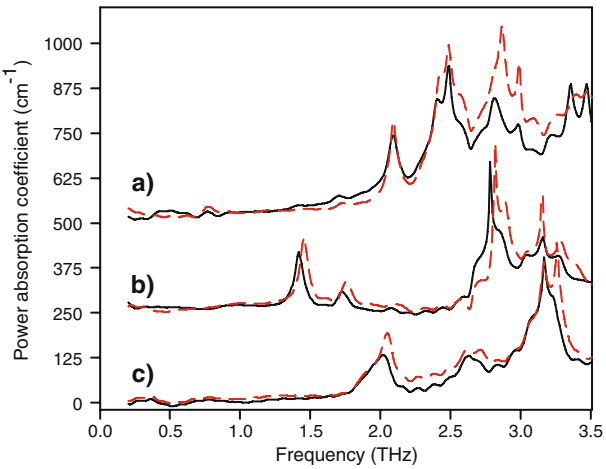

Fig. 5 THz spectra taken at 290 K (black solid lines) and 78 K (red dashed lines) for a) L-histidine (orthorhombic polymorph), b) D-histidine (monoclinic polymorph), and c) DL-histidine. Sets a) and b) have been vertically offset by 500 and 250 cm^{-1}, respectively.

50%-50% mixture of the metastable monoclinic and stable orthorhombic forms. The commercial D-histidine sample, in the metastable monoclinic form, also changes to an approximate 50%-50% mixture upon recrystallization. Low temperature (78 K) and room temperature (290 K) spectra are compared for all samples. At low temperature, peaks tend to sharpen and blue-shift.

Acknowledgements We acknowledge the National Science Foundation (CHE-0911593) and AstraZeneca for partial support of this work. KS thanks the German Academic Exchange Service (DAAD) for funding.

References

1. P. F. Taday, I. V. Bradley, D. D. Arnone, and M. Pepper, "Using terahertz pulse spectroscopy to study the crystalline structure of a drug: A case study of the polymorphs of ranitidine hydrochloride," J. Pharm. Sci. **92**, 831 (2003).
2. E. Pickwell and V. P. Wallace, "Biomedical applications of terahertz technology," J. Phys. D-Appl. Phys. **39**, R301 (2006).
3. C. J. Strachan, P. F. Taday, D. A. Newnham, K. C. Gordon, J. A. Zeitler *et al*., "Using terahertz pulsed spectroscopy to quantify pharmaceutical polymorphism and crystallinity," J. Pharm. Sci. **94**, 837 (2005).
4. P. C. Upadhya, K. L. Nguyen, Y. C. Shen, J. Obradovic, K. Fukushige *et al*., "Characterization of crystalline phase-transformations in theophylline by time-domain terahertz spectroscopy," Spectr. Lett. **39**, 215 (2006).
5. V. P. Wallace, P. F. Taday, A. J. Fitzgerald, R. M. Woodward, J. Cluff *et al*., "Terahertz pulsed imaging and spectroscopy for biomedical and pharmaceutical applications," Faraday Discuss. **126**, 255 (2004).
6. C. J. Strachan, T. Rades, D. A. Newnham, K. C. Gordon, M. Pepper *et al*., "Using terahertz pulsed spectroscopy to study crystallinity of pharmaceutical materials," Chem. Phys. Lett. **390**, 20 (2004).
7. G. A. Narvaez, J. Kim, and J. W. Wilkins, "Effects of morphology on phonons in nanoscopic silver grains," Phys. Rev. B **72**, 155411 (2005).
8. G. M. Day, J. A. Zeitler, W. Jones, T. Rades, and P. F. Taday, "Understanding the influence of polymorphism on phonon spectra: Lattice dynamics calculations and terahertz spectroscopy of carbamazepine," J. Phys. Chem. B **110**, 447 (2006).
9. J. C. Lee, H. Tazawa, T. Ikehara, and T. Nishi, "Crystallization kinetics and morphology in miscible blends of two crystalline polymers," Polym. J. **30**, 780 (1998).
10. E. Hendry, M. Koeberg, J. M. Schins, H. K. Nienhuys, V. Sundstrom *et al.*, "Interchain effects in the ultrafast photophysics of a semiconducting polymer: THz time-domain spectroscopy of thin films and isolated chains in solution," Phys. Rev. B **71** (2005).
11. R. Pantani, I. Coccorullo, V. Speranza, and G. Titomanlio, "Modeling of morphology evolution in the injection molding process of thermoplastic polymers," Prog. Polym. Sci. **30**, 1185 (2005).
12. Y. C. Shen, T. Lo, P. F. Taday, B. E. Cole, W. R. Tribe *et al*., "Detection and identification of explosives using terahertz pulsed spectroscopic imaging," Appl. Phys. Lett. **86**, 241116 (2005).
13. M. Yamaguchi, F. Miyamaru, K. Yamamoto, M. Tani, and M. Hangyo, "Terahertz absorption spectra of L-, D-, and DL-alanine and their application to determination of enantiometric composition," Appl. Phys. Lett. **86**, 053903 (2005).
14. T. M. Korter, R. Balu, M. B. Campbell, M. C. Beard, S. K. Gregurick *et al*., "Terahertz spectroscopy of solid serine and cysteine," Chem. Phys. Lett. **418**, 65 (2006).
15. C. P. M. Roelands, S. Jiang, M. Kitamura, J. H. terHorst, H. J. M. Kramer *et al*., "Antisolvent crystallization of the polymorphs of L-histidine as a function of supersaturation ratio and of solvent composition," Cryst. Growth Des. **6**, 955 (2006).
16. M. T. Averbuch-Pouchot, "Crystal structure of L-histidinium phosphite and a structure reinvestigation of the monoclinic form of L-histidine," Zeitschrift fuer Kristallographie **207**, 111 (1993).
17. M. S. Lehmann, T. F. Koetzle, and W. C. Hamilton, "Precision neutron-diffraction structure determination of protein and nucleic-acid components. 4. Crystal and molecular structure of amino acid L-Histidine," Int. J. Pept. Protein Res. **4**, 229 (1972).
18. F. H. Allen, "The Cambridge Structural Database: a quarter of a million crystal structures and rising," Acta Cryst. B **58**, 380 (2002).
19. C. F. Macrae, P. R. Edgington, P. McCabe, E. Pidcock, G. P. Shields *et al*., "Mercury: visualization and analysis of crystal structures," J. Appl. Crystallogr. **39**, 453 (2006).

20. A. Nahata, A. S. Weling, and T. F. Heinz, "A wideband coherent terahertz spectroscopy system using optical rectification and electro-optic sampling," Appl. Phys. Lett. **69**, 2321 (1996).
21. A. Rice, Y. Jin, X. F. Ma, X. C. Zhang, D. Bliss *et al*., "Terahertz optical rectification from (110) zincblende crystals," Appl. Phys. Lett. **64**, 1324 (1994).
22. Q. Wu, M. Litz, and X. C. Zhang, "Broadband detection capability of ZnTe electro-optic field detectors," Appl. Phys. Lett. **68**, 2924 (1996).
23. M. C. Beard, G. M. Turner, and C. A. Schmuttenmaer, "Transient photoconductivity in GaAs as measured by time- resolved terahertz spectroscopy," Phys. Rev. B **62**, 15764 (2000).
24. J. J. Madden, E. L. McGandy, and N. C. Seeman, "Crystal structure of monoclinic form of L-histidine," Acta Cryst. B **28**, 2382 (1972).
25. J. J. Madden, N. C. Seeman, and E. L. McGandy, "Crystal structure of orthorhombic form of L-(+)-histidine," Acta Cryst. B **28**, 2377 (1972).
26. P. Edington and M. M. Harding, "Crystal structure of DL-histidine," Acta Cryst. B **30**, 204 (1974).
27. R. Rungsawang, Y. Ueno, I. Tomita, and K. Ajito, "Angle-dependent terahertz time-domain spectroscopy of amino acid single crystals," J. Phys. Chem. B **110**, 21259 (2006).